

# Metagenomics analysis of the effects of *Agaricus bisporus* mycelia on microbial diversity and CAZymes in compost

Wanqiu Chang<sup>1,2</sup>, Weilin Feng<sup>2</sup>, Yang Yang<sup>3</sup>, Yingyue Shen<sup>2</sup>, Tingting Song<sup>2</sup>, Yu Li<sup>Corresp., 1</sup>, Weiming Cai<sup>Corresp. 2</sup>

<sup>1</sup> Jilin Agricultural University, Engineering Research Centre of Chinese Ministry of Education for Edible and Medicinal Fungi, Changchun, Jilin, China

<sup>2</sup> Zhejiang Academy of Agricultural Sciences, Institute of Horticulture, Hangzhou, Zhejiang, China

<sup>3</sup> Chinese Academy of Tropical Agricultural Sciences, Environment and Plant Protection Institute, Haikou, Hainan, China

Corresponding Authors: Yu Li, Weiming Cai

Email address: fungi966@126.com, caiwm527@126.com

*Agaricus bisporus* growth alters the lignocellulosic composition and structure of compost. However, it is difficult to differentiate the enzyme activities of *A. bisporus* mycelia from the wider microbial community owing to the complication of completely separating the mycelia from compost cultures. Macrogenomics analysis was employed in this study to examine the fermentation substrate of *A. bisporus* before and after mycelial growth, and the molecular mechanism of substrate utilization by *A. bisporus* mycelia was elucidated from the perspective of microbial communities and CAZymes in the substrate. The results showed that the relative abundance of *A. bisporus* mycelia increased by 77.57-fold after mycelial colonization, the laccase content was significantly increased and the lignin content was significantly decreased. Analysis of the CAZymes showed that AA10 family was extremely differentiated. Laccase-producing strains associated with AA10 family were mostly bacteria belonging to *Thermobifida* and *Thermostaphylospora*, suggesting that these bacteria may play a synergistic role in lignin decomposition along with *A. bisporus* mycelia. These findings provide preliminary evidence for the molecular mechanism of compost utilization by *A. bisporus* mycelia and offer a reference for the development and utilization of strains related to lignocellulose degradation.

# Metagenomics analysis of the effects of *Agaricus bisporus* mycelia on microbial diversity and CAZymes in compost

Wanqiu Chang<sup>1,2</sup>, Weilin Feng<sup>2</sup>, Yang Yang<sup>3</sup>, Yingyue Shen<sup>2</sup>, Tingting Song<sup>2</sup>, Yu Li<sup>1</sup> and Weiming Cai<sup>2</sup>

<sup>1</sup> Jilin Agricultural University, Engineering Research Centre of Chinese Ministry of Education for Edible and Medicinal Fungi, Changchun, Jilin, China

<sup>2</sup> Institute of Horticulture, Zhejiang Academy of Agricultural Sciences, Hangzhou, Zhejiang, China

<sup>3</sup> Environment and Plant Protection Institute, Chinese Academy of Tropical Agricultural Sciences, Haikou, Hainan, China

Corresponding Author:

Yu Li<sup>1</sup>, Jilin Agricultural University, Changchun, Jilin, 130118, China.

Email address: fungi966@126.com

Weiming Cai<sup>2</sup>, Zhejiang Academy of Agricultural Sciences, Hangzhou, Zhejiang, 310021, China.

Email address: caiwm527@126.com

## Abstract

*Agaricus bisporus* growth alters the lignocellulosic composition and structure of compost. However, it is difficult to differentiate the enzyme activities of *A. bisporus* mycelia from the wider microbial community owing to the complication of completely separating the mycelia from compost cultures. Metagenomics analysis was employed in this study to examine the fermentation substrate of *A. bisporus* before and after mycelial growth, and the molecular mechanism of substrate utilization by *A. bisporus* mycelia was elucidated from the perspective of microbial communities and CAZymes in the substrate. The results showed that the relative abundance of *A. bisporus* mycelia increased by 77.57-fold after mycelial colonization, the laccase content was significantly increased and the lignin content was significantly decreased. Analysis of the CAZymes showed that AA10 family was extremely differentiated. Laccase-producing strains associated with AA10 family were mostly bacteria belonging to *Thermobifida* and *Thermotaphylospora*, suggesting that these bacteria may play a synergistic role in lignin decomposition along with *A. bisporus* mycelia. These findings provide preliminary evidence for the molecular mechanism of compost utilization by *A. bisporus* mycelia and offer a reference for the development and utilization of strains related to lignocellulose degradation.

# Introduction

Agricultural biomass wastes comprise organic substances generated by humans during agricultural activities (Malool et al., 2021). As these wastes are produced in abundant quantities and pose disposal problems, there has been an increasing interest to develop efficient and safe strategies to utilize agricultural biomass waste (Sherwood, 2020, Grimm et al., 2018). At present, compost is still a primary mode of organic matter degradation (Wang et al., 2021).

Industrial-scale production of *Agaricus bisporus*, an edible mushroom with a long history of cultivation (Baars et al., 2020), has solved part of the problem of agricultural waste reuse to a certain extent (De Andrade et al., 2008). In the process of large-scale production of *A. bisporus*, agricultural wastes, such as wheat straw and chicken manure, are mainly used as raw materials for fermentation (Roncero-Ramos et al., 2017), which is both environmentally-friendly and economical, addressing the issue of reusing of agricultural waste to a certain extent (Colmenares-Cruz et al., 2017). In recent years, significant improvements in the *A. bisporus* cultivation process have been achieved, and the application of tunnel inoculation has altered the cultivation pattern and increased the mycelial growth rate. It has been reported that the localized tunnel-growth model achieved a 13.6% increase in *A. bisporus* growth rate, when compared with the cultivation house growth model (Wang et al., 2021). However, only a few studies have performed comparative investigations of inoculated and uninoculated mushroom compost. Some studies have suggested that *A. bisporus* mycelial growth produces a range of extracellular enzymes that are involved in the degradation of the lignocellulosic fraction in compost. Lignin is mainly degraded during *A. bisporus* mycelial growth stage (PIII), with an increase in guaiacyl lignin content (G-type lignin) (Wood et al., 1983), and the lignin-degradation products have been speculated to be the substrate for subsequent growth of *A. bisporus* (Jurak et al., 2015, Jurak et al., 2014). The decrease and changes in lignin during the mycelial growth stage can improve the digestibility of carbohydrates in the later growth phases. In a previous study, *A. bisporus* appeared to be the dominant fungal species based on visual observation of cropping beds; however, phospholipid fatty acid analysis (PLFA) conducted on mushroom compost revealed that *A. bisporus* mycelia accounted for 6.8% w/w of the mushroom compost after complete colonization, with only less than half of the mycelia being active (McGee et al., 2017).

Many studies have focused on the crucial role of bacteria and fungi in the degradation of organic compounds and their diverse modes of action on organic matter decomposition. While bacterial growth becomes restricted owing to their enhanced propagation on the surface of organic matter that acts as the main source of nutrients, the fungal hyphae have a strong penetrating ability. About concerning *Agaricus* growth, both mycelia and fruiting body production are not only dependent on the mushroom itself, but also bacteria and other fungi in the substrate, and the microbial community dynamics can completely change at the end of the composting process (Song et al., 2021). It has been noted that the final secondary fermentation (PII) compost mainly comprised lignocellulosic components from wheat straw together with microbial biomass (Martínez et al., 2008). Pasteurization of the compost material before inoculation has been found to result in the predominance of fungal community in the substrate, with *A. bisporus*

becoming the major fungal strain and its mycelia subsequently colonizing the substrate by degrading the organic material to release nutrients (McGee, 2018). However, little is known about the composition and activity of the wider fungal community in the compost substrate besides *A. bisporus* throughout the mushroom cultivation process. Therefore, the present study aimed to reveal the utilization of compost substrate before and after *A. bisporus* mycelial growth and compare the differences in the microbial communities and enzyme families in the compost. Furthermore, the effects of *A. bisporus* mycelial growth on other microorganisms during large-scale cultivation of *A. bisporus* were determined to identify novel microorganisms with potential roles in lignin degradation.

## Materials & Methods

### Sample collection and DNA extraction

Commercial strain A15 of *A. bisporus* from Sylvan (USA) was used in this study and stored in the Engineering Research Center of Chinese Ministry of Education for Edible and Medicinal Fungi (ERCCMEEMF) at Jilin Agricultural University (Changchun, China). The compost fermentation and mycelial culture experiments were performed at Zhejiang Longchen Modern Agricultural Science and Technology Co. Ltd, Jiaxing City, Zhejiang Province, China. The compost comprised wheat straw (90 t), chicken manure (83 t), peanut meal (3 t), and gypsum (9 t). Peanut meal was added as an auxiliary nitrogen source because the components of wheat straw and chicken manure in China were different from those in Europe and America (Jun et al., 2021). Before commencing compost fermentation, the initial C/N ratio of the compost was adjusted to 25:1. The straws were completely dampened and piled up for 1–3 days, and then the other materials were mixed and piled again for 2–3 days. The pre-compost was placed into the tunnel for primary fermentation (PI) (Straatsma et al., 2000, Mouthier et al., 2017). The pile was turned three times on days 2, 4, and 7, respectively. The treatment parameters were adjusted based on compost temperature to allow the material temperature to reach 70°C–80°C and remain constant for 6 days (P I). Immediately after that, secondary fermentation (Compost-P II) was conducted for 6–7 days by pasteurization (Vieira et al., 2018). After secondary fermentation, inoculation was performed when the temperature decreased to 24°C and NH<sub>3</sub> level was ≤10 mg/L (Sharma et al., 2005). The temperature, humidity, air pressure, air volume, and other environmental factors were adjusted using Dutch Christiaens Group equipment for the intelligent control system. Under optimal environmental conditions, *A. bisporus* mycelia could grow all over the compost after 18 days (Mycelium-P III) (Iiyama et al., 1994).

Subsequently, samples were collected from the uninoculated compost and mycelia-filled compost, respectively. Before sample collection, the composts in the top, middle, and bottom layers of the reactor were fully mixed (Meng et al., 2021). All the samples were divided into two parts: one part was stored at 4°C for physicochemical analysis and the other was frozen at –80°C for DNA extraction. The genomic DNA was extracted from the samples using an Omega EZNA soil DNA kit, and the integrity, purity, and concentration of the extracted genomic DNA were

examined by 1% agarose gel electrophoresis (100 V, 1.5 h), NanoDrop 2000, and Qubit 3.0, respectively. The extracted DNA was stored in an ultra-low-temperature freezer at  $-20^{\circ}\text{C}$  and transported to OE Biomedical Technology (Shanghai, China) for sequencing.

### **Analysis of compost physicochemical properties**

The compost samples were dried in an oven at  $105^{\circ}\text{C}$  for 5 h to assess the moisture content. The dried samples were crushed and placed in the control box of a resistance furnace at  $600^{\circ}\text{C}$  for 2 h to determine the ash content. The total nitrogen (Total-N) and carbon (Total-C) content in the samples were determined using the Kjeldahl method and  $\text{K}_2\text{Cr}_2\text{O}_3$  oxidation. Determination of the pH values with an electronic pH meter (Mettler-Toledo Instruments Co., Ltd., Shanghai, China) using 10%(w/v) sample suspensions were used. Laccase and xylanase activities in the samples were evaluated using a Solarbio kit, and lignin, cellulose, and hemicellulose components were determined according to Van Soes method.

### **Metagenome sequencing, assembly, and annotation**

Metagenome sequencing was accomplished using the Illumina HiSeq platform with a 500-bp sequencing library. The raw data (raw reads) quality was pre-processed using Trimmomatic (Bolger *et al.*, 2014) software, and optimized sequences were spliced and assembled using MEGAHIT (Li *et al.*, 2015, Li *et al.*, 2016) software based on De-Bruijn graph principle, and contigs with length  $< 500$  bp were filtered out for subsequent analysis. The open reading frame (ORF) of the spliced contigs was predicted with Prodigal software (Hyatt *et al.*, 2010). CD-HIT software was adopted to remove redundant and non-redundant initial unigenes. The clustering parameters included 95% identity and 90% coverage. The clean reads of each sample were aligned to the non-redundant genes set (95% identity) using bowtie 2 software to calculate the gene abundance in the corresponding samples. The representative sequences in the non-redundant unigenes set were annotated to the obtained species information according to the best alignment attained by BLASTP (E value  $< 1\text{e-}5$ ) to National Center for Bio-technology Information (NCBI) Non-Redundant Database (Nr). Then, the sum of gene abundances for the corresponding species was used to calculate species abundance.

### **Identification of carbohydrate-active enzymes**

To evaluate the carbon utilization potential of microbial communities during *A. bisporus* mycelial growth, the non-redundant genes were compared with the carbohydrate-active enzymes database (CAZy) using DIAMOND software ( $e < 1\text{e-}5$ ) (Buchfink *et al.*, 2015). First, all proteins with the highest sequence similarity were screened and subjected to CAZy to search against sequence libraries with the families of glycoside hydrolases (GHs), auxiliary activities (AAs), carbohydrate-binding modules (CBMs), glycosyltransferases (GTs), polysaccharide lyases (PLs), and carbohydrate esterases (CEs). Then, the differences in the CAZyme family between the two samples (uninoculated compost and mycelia-filled compost) were compared and analyzed (Donhauser *et al.*, 2021).

### **Data and statistical analyses**

Raw data were entered and stored in Excel. The differences among the samples were examined by independent samples *t*-tests with statistical significance at  $p < 0.05$  and  $p < 0.01$ . The data are presented as mean  $\pm$  standard deviation (SD). GraphPad Prism 8.0 software and Origin

were applied for statistical analysis and plotting, and a cloud platform (<http://www.cloudtutu.com/>) was employed for plotting.

# Results

## Physicochemical properties of Compost-PII and Mycelium-PIII

After completion of PII, the material temperature was reduced using fans. Subsequently, *A. bisporus* was inoculated (4% (w/w)) and the compost substrate was filled with mycelial growth after 18 days of incubation at 22 °C–24 °C. During this period, the water content in the compost decreased from 66.48% to 61.77% with the increase in mycelial growth, whereas the ash content increased by 1.71%(Table 1). It must be noted that the water content can affect microbial activities, which in turn can influence enzyme activities. During *A. bisporus* mycelial growth, carbon consumption predominantly increased, whereas nitrogen utilization was relatively less maintained at 2.12-2.13% and no significant difference(Table 1). After mycelial growth, the pH of the compost decreased from 7.80 to 6.27. Analysis of the cellulose and lignin contents in the compost by Van Soes method revealed that the cellulose content and lignin content significantly decreased(Fig. 1). Furthermore, evaluation of the activities of several known carbon-source-degradation-related enzyme families indicated a moderate increase in xylanase and laccase activities after *A. bisporus* mycelial growth, 3-fold and 15-fold increase respectively(Figs. 2B & 2C). The solubility of lignin in aqueous solutions was low, and the decrease in the pH of the culture material may have a significant effect on lignin solubility. In addition, the increase in protease(Fig. 2D) also promotes better development of the mycelium(Wang *et al.*, 2021).

## Diversity of microbial communities in Compost-PII and Mycelium-PIII

The effective data volume of each sample in this experiment was 11.23-17.22 G. The N50 statistics of Contigs were distributed between 1631-2349 bp, and the number of OFR in the set of non-redundant genes was 1029162 after redundancy. The annotation rates were 89.44%, 74.62%, 42.21% and 2.57% for the non-redundant genes compared with NR, eggNOG, KEGG and CAZy databases respectively. Metagenomics analysis indicated the dominance of bacterial community in Compost-PII and Mycelium-PIII samples (93.17% and 94.27%, respectively), followed by fungi (0.25% and 0.29%, respectively), whereas the archaeal abundance remained almost unchanged. However, the abundance of viruses declined with *A. bisporus* mycelial growth (1.18% in Compost-PII and 0.13% in Mycelium-PIII). A total of 181 phyla, 157 classes, 805 families, 3460 genera, and 22,567 species were detected in the samples. The six most prominent bacterial phyla were Proteobacteria, Actinobacteria, Chloroflexi, Planctomycetes, Bacteroidetes, and Firmicutes(Zhang *et al.*, 2014), and the abundances of Actinobacteria and Planctomycetes significantly increased after *A. bisporus* mycelial growth(Fig. 3A). Intriguingly, numerous lignocellulose-decomposing bacteria have been reported to belong to Proteobacteria, Firmicutes, Actinobacteria, and Bacteroidetes(Lewin *et al.*, 2013, Pankratov *et al.*, 2011). Proteobacteria and Bacteroidetes are known to play a major role in organic matter degradation and C cycling (Wang *et al.*, 2018), and Bacteroidetes can break down lignocellulose into short-chain fatty acids (Dodd *et al.*, 2011). It is noteworthy that although the relative abundance of the Basidiomycota phylum was low, it showed

a great increase(Fig. 3B).

# **Analysis of bacterial and fungal communities**

In the present study, *Thermobifida*, *Thermostaphylospora*, *Sphaerobacter*, *Thermopolyspora*, *Pseudoxanthomonas*, and *Rhodothermus* were the predominant bacterial genera in the Compost-PII and Mycelium-PIII samples(Cao *et al.*, 2019, Durrant *et al.*, 1991). When compared with the Compost-PII samples, the relative abundances of *Thermobifida*, *Thermostaphylospora*, *Sphaerobacter*, *Thermomonospora*, and *Chelatococcus* were significantly increased in Mycelium-PIII samples; in contrast, the relative abundances of *Thermopolyspora*, *Rhodothermus*, and *Pseudoxanthomonas* presented the opposite trend (Fig. 4A). Analyses of the microbial community composition confirmed significant shifts in the microbial community structure between the two groups, and many of the enriched genera also co-varied with function. Moreover, the variability of these microbial communities may be correlated with nutrients, compost temperature, moisture content, and pH.

At the species level, the relative abundance of *A. bisporus* presented the highest increase among fungi, exhibiting a 77.57-fold increase after complete mycelial growth (Figs. 4D). In addition to *A. bisporus*, the activities of other microorganisms, such as the bacteria (Figs. 4C) *Thermostaphylospora\_chromogena*, *Thermomonospora\_sp.\_CIF\_1*, *Sandaracinaceae\_bacterium*, and *Chelatococcus\_composti*, and fungi (Figs.4D) *Spizellomyces\_punctatus*, *Rozella\_allomyis*, and *Basidiobolus\_meristosporus*, were also enhanced during *A. bisporus* mycelial growth.

# **Analysis of CAZymes**

The carbon-utilization potential of the microbial communities in the compost was assessed to evaluate the effects of altered substrate quantity and quality resulting from the shift in microbial activity during *A. bisporus* mycelial growth. Among the genes annotated with CAZy, in total, 431 different CAZyme families (229 GHs, 81 GTs, 48 PLs, 17 AAs, 16 CEs, and 40 CBMs) were detected in the samples. The most abundant enzyme classes at all temperatures were GHs and GTs, whereas those with the lowest abundance were PLs and AAs. At the family level, GTs were especially abundant in all the samples, with GT2 (cellulose/chitin synthase and other functions), GT4 (sucrose synthase and other functions), and GT83 (galacturonosyl transferase and other functions) being the most abundant (Paixão *et al.*, 2021, Leadbeater *et al.*, 2021).

Cellulose, hemicellulose, and lignin are major constituents of lignocellulose-containing raw materials (Stech *et al.*, 2014). In the present study, cellulose- and hemicellulose-degrading enzymes exhibited the highest activities in Compost-PII and Mycelium-PIII samples, with GH5, GH8, and GH9 families being the predominant cellulose-degrading enzymes and GH2, GH10, GH11, GH26, and GH53 families being the major hemicellulose-degrading enzymes(Table 2). The GH2 family includes multiple enzymes, and it has been demonstrated that  $\alpha$ -1,3-L-arabinofuranosidase activity on substituted xylan does not improve compost degradation by *A. bisporus*. In nature, it is generally attributed to the metabolism of basidiomycetes white-rot fungi, since they degrade lignin more rapidly and extensively than other microorganisms(Woiciechowski *et al.*, 2013). Although not a wood-rotting fungus, the *Agaricus bisporus* still plays a key role in the degradation of lignin as a grass-rotting fungus. Although AA7 family genes have been reported

to play a role in lignin degradation (Andlar et al., 2018) and the content of these genes was relatively high in the lignin-degradation-related enzymes family in the present study, this enzymes family was not significantly different. There is a large content of the AA3 and AA6 enzyme families associated with lignin breakdown (Table 2).

### Variations in enzyme families between Compost-PII and Mycelium-PIII

The effect of *A. bisporus* mycelium on the compost substrate was mainly reflected in the enzyme families with low relative abundance at the population level. For instance, the abundances of GT32 and GH24 significantly decreased, whereas those of GH42, AA10, and CBM13 significantly increased. Furthermore, the abundance of GH8 presented a slight decrease (Figs. 5A). GH24 is known to act in association with lysozyme, GH8 is the main family of enzymes involved in cellulose degradation, and GH42 plays an important role in hemicellulose degradation. *Thermotaphylospora* belonging to Actinobacteria mainly causes an increase in the activities of  $\beta$ -galactosidase and  $\alpha$ -L-arabylanosidase of the GH42 family in the galactose metabolism pathway during the mycelial growth stage, and CBM67 has been reported to exhibit  $\alpha$ -L-rhamnose-binding activity (Fujimoto et al., 2013).

In the present study, the increase in the laccase content during the mycelial growth stage was mainly related to the AA10 family (Table 2). The major strains that cause differential laccase production are *Thermobifida*, *Thermotaphylospora*, and *Cellulomonas*, and in the present study, the relative abundances of *Thermobifida* and *Cellulomonas* decreased, while that of *Thermotaphylospora* increased (Figs. 5B&5C). Furthermore, the increase in the xylanase content during *A. bisporus* mycelial growth stage was mainly related to the CBM13 family, and *Thermotaphylospora* was also the dominant genus that caused this increase (Figs. 5D&5E).

## Discussion

Degradation of lignin during the composting process has been reported to be caused by certain fungi and several species of bacteria and Actinomycetes (Kabel et al., 2017, Fermor et al., 1981, Del Cerro et al., 2021, Ayuso-Fernández et al., 2018). In the present study, the artificial introduction of *A. bisporus* at the end of the composting process and the resultant dominance of *A. bisporus* in the fungal community played a major role in lignin degradation. A similar finding has also been reported by Jean-Michel Savoie et al. (Savoie, 1998, Zhang et al., 2019). During the mycelial growth of *A. bisporus*, the oxidative phosphorylation pathway became dominant, which subsequently affected the bacterial and fungal communities composition, and a part of lignin degradation originated from bacterial action. Jurak et al. showed that xylan solubility increased by 20% during mycelial growth, indicating partial degradation of the xylan skeleton. In the present study, xylan degradation was mainly associated with the action of *Thermotaphylospora*. However, despite xylan degradation, the carbohydrate composition and degree of substitution of xylan in the compost at the beginning and end of the mycelial growth stage were rather similar (Jurak et al., 2014). The protease activity that was measured had an increasing trend. This might imply that after accessing the mycelium of *Agaricus bisporus*, the raw material chicken manure and wheat straw were used for the breakdown of the macromolecular nitrogen source material and



subsequently for the development and growth of their mycelium(Wang *et al.*, 2021).

In a previous study, some researchers(Zhang *et al.*, 2014) determined the rRNA gene copy number of Actinomycetes and fungi during the composting process by quantitative PCR, and found that the fungal genus *Agaricus* and unknown fungal community accounted for 45% and 55% of the microbial community, respectively, while the bacterial genus *Streptomyces* accounted for 60% of the total bacterial community during the mycelial growth phase. In contrast, in the present study, although the abundance of *Streptomyces* varied before and after the mycelial growth stage, the difference was not significant. Moreover, besides *Agaricus*, *Basidiobolus* and *Spizellomyces* were also the predominant fungi, thus providing further insights into the composition of the fungal community in the compost.

During the *A. bisporus* mycelial growth stage, the relative abundances of gene sequences still remained high at high-temperature composting, and although the abundance of fungal communities increased, the number of bacterial genes was much higher than that of fungal genes. However, as it was not possible to determine the number of active bacteria during this stage, microbial communities with a higher relative abundance of gene sequences were compared, and *A. bisporus* was found to be dominant in the fungal community. While enzymes related to lignocellulose breakdown were not detected in the macrogenome of *A. bisporus*, analysis of whole-genome data of *A. bisporus* substrate confirmed the presence of a large number of genes encoding lignocellulose-degrading enzymes(Morin *et al.*, 2012), because macrogenome sequencing results did not assemble genes encoding lignocellulose-degrading enzymes in *A. bisporus*. Moreover, variations were also noted in the expression of genes encoding CAZymes between compost-grown mycelia and fruiting body, with genes encoding plant cell wall degrading enzymes detected in compost-grown mycelia, but largely undetected in the fruiting body. Similarly, Patyshakuliyeva *et al.* also confirmed that compost-grown mycelia could express a large variety of CAZyme genes related to the degradation of plant biomass components(Patyshakuliyeva *et al.*, 2013). In addition, transcriptomics and proteomics investigations performed in a previous study also demonstrated that genes related to lignin degradation were only highly expressed on day 16 of mycelial growth, indicating that lignin was degraded at the initial stage of mycelial growth and was no longer altered after complete growth of mycelia (Patyshakuliyeva *et al.*, 2015). Moreover, compost-grown mycelia were found to express a large number of CAZymes-encoding genes associated with the degradation of plant biomass components. In summary, the present study uncovered lignocellulose-degrading microorganisms and enzyme expressions in bacteria during *A. bisporus* mycelial growth stage in the composting process, providing further insights into lignin degradation in compost. Lignin degradation was mostly bacteria, and the main laccase-producing bacteria belonged to *Thermobifida* (Mironov *et al.*, 2021, Vanee *et al.*, 2017)and *Thermostaphylospora*, with *Thermostaphylospora* presenting a significant increase. The results obtained can further strengthen our understanding of the specificity of *A. bisporus* mycelial growth.

## Conclusions

The present study found the laccase content was increased during the *A. bisporus* mycelial

growth stage. Laccases belonging to the AA10 family were mainly derived from *Thermobifida* and *Thermostaphylospora*, the potential for lignin-degrading enzymes of bacterial origin may be grossly underestimated. *Agaricus* proliferation may require an interacting consortium of both bacteria and fungi for effective lignocellulose degradation. The results obtained offer insights into the difference in enzyme activities between *A. bisporus* mycelia and other microbial communities, and enhance our understanding of the changes in microbial communities and enzyme families during *A. bisporus* mycelial growth phase in the composting process.

## References

- Malool ME, Keshavarz Moraveji M, Shayegan J. 2021. Optimized production, Pb(II) adsorption and characterization of alkali modified hydrochar from sugarcane bagasse. *Scientific Reports* **11**:22328-22328. DOI 10.1038/s41598-021-01825-y.
- Sherwood J. 2020. The significance of biomass in a circular economy. *Bioresource Technology* **300**:122755. DOI 10.1016/j.biortech.2020.122755.
- Grimm D, Wösten HAB. 2018. Mushroom cultivation in the circular economy. *Applied Microbiology and Biotechnology* **102**:7795-7803. DOI 10.1007/s00253-018-9226-8.
- Wang WK, Liang CM. 2021. Enhancing the compost maturation of swine manure and rice straw by applying bioaugmentation. *Scientific Reports* **11**:6103. DOI 10.1038/s41598-021-85615-6.
- Baars JJP, Scholtmeijer K, Sonnenberg ASM, van Peer AV. 2020. Critical Factors Involved in Primordia Building in *Agaricus bisporus*: A Review. *Molecules* **25**:2984. DOI 10.3390/molecules25132984.
- De Andrade MC, Zied DC, De Almeida Minihoni MT, Kopytowski Filho J. 2008. Yield of four *Agaricus bisporus* strains in three compost formulations and chemical composition analyses of the mushrooms. *Braz J Microbiology* **39**:593-598. DOI 10.1590/s1517-838220080003000034.
- Roncero-Ramos I, Delgado-Andrade C. 2017. The beneficial role of edible mushrooms in human health. *Current Opinion in Food Science* **14**:122-128. DOI 10.1016/j.cofs.2017.04.002.
- Colmenares-Cruz S, Sánchez JE, Valle-Mora J. 2017. *Agaricus bisporus* production on substrates pasteurized by self-heating. *Amb Express* **7**:135. DOI 10.1186/s13568-017-0438-6.
- Wang Q, Xiao TT, Song XX, Shen XF, Jun JX, Zhang JX, Chen H, Huang JC. 2021. Effects of Running Phase III in a Tunnel on *Agaricus bisporus* mycelial growth and compost degradation. *Acta Edulis Fungi* **28**:86-92. DOI 10.16488/j.cnki.1005-9873.2021.03.011.
- Wood DA, Leatham GF. 1983. Lignocellulose degradation during the life cycle of *Agaricus bisporus*. *FEMS Microbiology Letters* **20**:421-424. DOI 10.1111/j.1574-6968.1983.tb00160.x.
- Jurak E, Punt AM, Arts W, Kabel MA, Gruppen H. 2015. Fate of Carbohydrates and Lignin during Composting and Mycelium Growth of *Agaricus bisporus* on Wheat Straw Based Compost. *PLoS One* **10**:1-16. DOI 10.1371/journal.pone.0138909.
- Jurak E, Kabel MA, Gruppen H. 2014. Carbohydrate composition of compost during composting and mycelium growth of *Agaricus bisporus*. *Carbohydrate Polymers* **101**:281-288. DOI 10.1016/j.carbpol.2013.09.050.
- McGee, Conor F. 2017. Microbial ecology of the *Agaricus bisporus* mushroom cropping process. *Applied Microbiology and Biotechnology* **102**:1075-1083. DOI 10.1007/s00253-017-8683-9.
- Song TT, Shen YY, Jin QL, Feng WL, Fan LJ, Cao GT, Cai WM. 2021. Bacterial community diversity,

- lignocellulose components, and histological changes in composting using agricultural straws for *Agaricus*  
*bisporus* production. *PeerJ* **9**:e10452. DOI 10.7717/peerj.10452.
- Martínez áT, Rencoret J, Marques G, Gutiérrez A, Ibarra D, Jiménez-Barbero J, Río J. 2008.** Monolignol  
acylation and lignin structure in some nonwoody plants: A 2D NMR study. *Phytochemistry* **69**:2831-2843.  
DOI 10.1016/j.phytochem.2008.09.005.
- McGee CF. 2018.** Microbial ecology of the *Agaricus bisporus* mushroom cropping process. *Applied Microbiology  
and Biotechnology* **102**:1075-1083. DOI 10.1007/s00253-017-8683-9.
- Jun JX, Song XX, Xiao TT, Huang JC, Wang Q, Chen H, Zhang JJ, Chen MJ. 2021.** Screening of Phase 3  
Compost formula for Industrial Cultivation of *Agaricus bisporus* with Rice Straw. *Acta Edulis Fungi* **28**:80-  
86. DOI 10.16488/j.cnki.1005-9873.2021.06.011.
- Straatsma G, Gerrits JPG, Thissen JTNM, Amsing JGM, Loeffen H, Van Griensven LJLD. 2000.** Adjustment  
of the composting process for mushroom cultivation based on initial substrate composition. *Bioresource  
Technology* **72**:67-74. DOI 10.1016/S0960-8524(99)00088-7.
- Mouthier TMB, Kilic B, Vervoort P, Gruppen H, Kabel MA. 2017.** Potential of a gypsum-free composting process  
of wheat straw for mushroom production. *PLoS One* **12**:e0185901. DOI 10.1371/journal.pone.0185901.
- Vieira FR, Pecchia JA. 2018.** An Exploration into the Bacterial Community under Different Pasteurization  
Conditions during Substrate Preparation (Composting–Phase II) for *Agaricus bisporus* Cultivation.  
*Microbial Ecology* **75**:318-330. DOI 10.1007/s00248-017-1026-7.
- Sharma S, Lyons G, Chambers J. 2005.** Comparison of the changes in mushroom (*Agaricus bisporus*) compost  
during windrow and bunker stages of phase I and II. *Annals of Applied Biology* **136**:59-68. DOI  
10.1111/j.1744-7348.2000.tb00009.x.
- Iiyama K, Stone BA, Macauley BJ. 1994.** Compositional Changes in Compost during Composting and Growth of  
*Agaricus bisporus*. *Applied Microbiology and Biotechnology* **60**:1538-1546. DOI 10.1128/aem.60.5.1538-  
1546.1994.
- Meng L, Li W, Zhang S, Zhang X, Zhao Y, Chen L. 2021.** Improving sewage sludge compost process and quality  
by carbon sources addition. *Scientific Reports* **11**:1319. DOI 10.1038/s41598-020-79443-3.
- Bolger AM, Lohse M, Usadel B. 2014.** Trimmomatic: a flexible trimmer for Illumina sequence data. *Bioinformatics*  
**30**:2114-2120. DOI 10.1093/bioinformatics/btu170.
- Li D, Liu CM, Luo R, Sadakane K, Lam TW. 2015.** MEGAHIT: an ultra-fast single-node solution for large and  
complex metagenomics assembly via succinct de Bruijn graph. *Bioinformatics* **31**:1674-1676. DOI  
10.1093/bioinformatics/btv033.
- Li D, Luo R, Liu CM, Leung CM, Ting HF, Sadakane K, Yamashita H, Lam TW. 2016.** MEGAHIT v1.0: A fast  
and scalable metagenome assembler driven by advanced methodologies and community practices. *Methods*  
**102**:3-11. DOI 10.1016/j.ymeth.2016.02.020.
- Hyatt D, Chen GL, Locascio PF, Land ML, Larimer FW, Hauser LJ. 2010.** Prodigal: prokaryotic gene recognition  
and translation initiation site identification. *BMC Bioinformatics* **11**:119. DOI 10.1186/1471-2105-11-119.
- Buchfink B, Xie C, Huson DH. 2015.** Fast and sensitive protein alignment using DIAMOND. *Nat Methods* **12**:59-  
60. DOI 10.1038/nmeth.3176.
- Donhauser J, Qi W, Bergk-Pinto B, Frey B. 2021.** High temperatures enhance the microbial genetic potential to  
recycle C and N from necromass in high-mountain soils. *Global Change Biology* **27**:1365-1386. DOI  
10.1111/gcb.15492.

- 399 **Wang Q, Juan JX, Xiao TT, Zhang JJ, Chen H, Song XX, Chen MJ, Huang JC. 2021.** The physical structure of  
400 compost and C and N utilization during composting and mushroom growth in *Agaricus bisporus* cultivation  
401 with rice, wheat, and reed straw-based composts. *Applied Microbiology Biotechnology* **105**:3811-3823. DOI  
402 10.1007/s00253-021-11284-0.
- 403 **Zhang X, Zhong YH, Yang SD, Zhang WX, Liu WF. 2014.** Diversity and dynamics of the microbial community  
404 on decomposing wheat straw during mushroom compost production. *Bioresource Technology* **170**:183-195.  
405 DOI 10.1016/j.biortech.2014.07.093.
- 406 **Lewin A, Wentzel A, Valla S. 2013.** Metagenomics of microbial life in extreme temperature environments. *Current*  
407 *Opinion in Biotechnology* **24**:516-525. DOI 10.1016/j.copbio.2012.10.012.
- 408 **Pankratov TA, Ivanova AO, Dedysh SN, Liesack W. 2011.** Bacterial populations and environmental factors  
409 controlling cellulose degradation in an acidic Sphagnum peat. *Environmental Microbiology* **13**:1800-1814.  
410 DOI 10.1111/j.1462-2920.2011.02491.x.
- 411 **Wang K, Mao H, Li X. 2018.** Functional characteristics and influence factors of microbial community in sewage  
412 sludge composting with inorganic bulking agent. *Bioresource Technology* **249**:527-535. DOI  
413 10.1016/j.biortech.2017.10.034.
- 414 **Dodd D, Mackie RI, Cann IK. 2011.** Xylan degradation, a metabolic property shared by rumen and human colonic  
415 Bacteroidetes. *Molecular Microbiology* **79**:292-304. DOI 10.1111/j.1365-2958.2010.07473.x.
- 416 **Cao GT, Song TT, Shen YY, Jin QL, Cai WM. 2019.** Diversity of Bacterial and Fungal Communities in Wheat  
417 Straw Compost for *Agaricus bisporus* Cultivation. *HortScience: a publication of the American Society for*  
418 *Horticultural Science* **54**:100-109. DOI 10.21273/HORTSCI13598-18.
- 419 **Durrant AJ, Wood DA, Cain RB. 1991.** Lignocellulose biodegradation by *Agaricus bisporus* during solid substrate  
420 fermentation. *Microbiology* **137**:751-755. DOI 10.1099/00221287-137-4-751.
- 421 **Paixão DAA, Tomazetto G, Sodré VR, Gonçalves TA, Uchima CA, Büchli F, Alvarez TM, Persinoti GF, Da**  
422 **Silva MJ, Bragatto J, Liberato MV, Franco Cairo JPL, Leme AFP, Squina FM. 2021.** Microbial  
423 enrichment and meta-omics analysis identify CAZymes from mangrove sediments with unique properties.  
424 *Enzyme and Microbial Technology* **148**:109820. DOI 10.1016/j.enzmictec.2021.109820.
- 425 **Leadbeater DR, Oates NC, Bennett JP, Li Y, Dowle AA, Taylor JD, Alponi JS, Setchfield AT, Alessi AM,**  
426 **Helgason T, McQueen-Mason SJ, Bruce NC. 2021.** Mechanistic strategies of microbial communities  
427 regulating lignocellulose deconstruction in a UK salt marsh. *Microbiome* **9**:48. DOI 10.1186/s40168-020-  
428 00964-0.
- 429 **Stech M, Hust M, Schulze C, Dübel S, Kubick S. 2014.** Cell-free eukaryotic systems for the production, engineering,  
430 and modification of scFv antibody fragments. *ENGINEERING IN LIFE SCIENCES* **14**:387-398. DOI  
431 10.1002/elsc.201400036.
- 432 **Woiciechowski AL, Vandenberghe LPDS, Karp SG, Letti L, Soccol CR. 2013.** The Pretreatment Step in  
433 Lignocellulosic Biomass Conversion: Current Systems and New Biological Systems. *Lignocellulose*  
434 *Conversion*:39-64. DOI 10.1007/978-3-642-37861-4\_3.
- 435 **Andlar M, Rezić T, Marđetko N, Kracher D, Ludwig R, Šantek B. 2018.** Lignocellulose degradation: An overview  
436 of fungi and fungal enzymes involved in lignocellulose degradation. *Engineering in life science* **18**:768-778.  
437 DOI 10.1002/elsc.201800039.
- 438 **Fujimoto Z, Jackson A, Michikawa M, Maehara T, Momma M, Henrissat B, Gilbert HJ, Kaneko S. 2013.** The  
439 structure of a *Streptomyces avermitilis*  $\alpha$ -L-rhamnosidase reveals a novel carbohydrate-binding module

- CBM67 within the six-domain arrangement. *Journal of biological chemistry* **288**:12376-12385. DOI 10.1074/jbc.M113.460097.
- Kabel MA, Jurak E, Mäkelä MR, De Vries RP. 2017.** Occurrence and function of enzymes for lignocellulose degradation in commercial *Agaricus bisporus* cultivation. *Applied Microbiology and Biotechnology* volume **101**:4363-4369. DOI 10.1007/s00253-017-8294-5.
- Fermor TR, Wood DA. 1981.** Degradation of Bacteria by *Agaricus bisporus* and Other Fungi. *Microbiology* **126**:377-387. DOI 10.1099/00221287-126-2-377.
- Del Cerro C, Erickson E, Dong T, Wong AR, Eder EK, Purvine SO, Mitchell HD, Weitz KK, Markillie LM, Burnet MC, Hoyt DW, Chu RK, Cheng JF, Ramirez KJ, Katahira R, Xiong W, Himmel ME, Subramanian V, Linger JG, Salvachúa D. 2021.** Intracellular pathways for lignin catabolism in white-rot fungi. *Proc Natl Acad Sci U S A* **118**:e2017381118. DOI 10.1073/pnas.2017381118.
- Ayuso-Fernández I, Ruiz-Dueñas FJ, Martínez AT. 2018.** Evolutionary convergence in lignin-degrading enzymes. *Proc Natl Acad Sci U S A* **115**:6428-6433. DOI 10.1073/pnas.1802555115.
- Savoie J-M. 1998.** Changes in enzyme activities during early growth of the edible mushroom, *Agaricus bisporus*, in compost. *Mycological Research* **102**:1113-1118. DOI 10.1017/S0953756298006121.
- Zhang HL, Wei JK, Wang QH, Yang R, Gao XJ, Sang YX, Cai PP, Zhang GQ, Chen QJ. 2019.** Lignocellulose utilization and bacterial communities of millet straw based mushroom (*Agaricus bisporus*) production. *Scientific Reports* **9**:1151. DOI 10.1038/s41598-018-37681-6.
- Morin E, Kohler A, Baker AR, Foulongne-Oriol M, Lombard V, Nagy LG, Ohm RA, Patyshakuliyeva A, Brun A, Aerts AL, Bailey AM, Billette C, Coutinho PM, Deakin G, Doddapaneni H, Floudas D, Grimwood J, Hildén K, Kües U, Labutti KM, Lapidus A, Lindquist EA, Lucas SM, Murat C, Riley RW, Salamov AA, Schmutz J, Subramanian V, Wösten HA, Xu J, Eastwood DC, Foster GD, Sonnenberg AS, Cullen DD, De Vries RP, Lundell T, Hibbett DS, Henrissat B, Burton KS, Kerrigan RW, Challen MP, Grigoriev IV, Martin F. 2012.** Genome sequence of the button mushroom *Agaricus bisporus* reveals mechanisms governing adaptation to a humic-rich ecological niche. *Proc Natl Acad Sci USA* **109**:17501-17506. DOI 10.1073/pnas.1206847109.
- Patyshakuliyeva A, Jurak E, Kohler A, Baker A, Battaglia E, De Bruijn W, Burton KS, Challen MP, Coutinho PM, Eastwood DC, Gruben BS, Mäkelä MR, Martin F, Nadal M, Van Den Brink J, Wiebenga A, Zhou M, Henrissat B, Kabel M, Gruppen H, De Vries RP. 2013.** Carbohydrate utilization and metabolism is highly differentiated in *Agaricus bisporus*. *BMC Genomics* **14**:663. DOI 10.1186/1471-2164-14-663.
- Patyshakuliyeva A, Post H, Zhou M, Jurak E, Heck AJ, Hildén KS, Kabel MA, Mäkelä MR, Altelaar MA, De Vries RP. 2015.** Uncovering the abilities of *Agaricus bisporus* to degrade plant biomass throughout its life cycle. *Environmental microbiology* **17**:3098-3109. DOI 10.1111/1462-2920.12967.
- Mironov V, Vanteeva A, Sokolova D, Merkel A, Nikolaev Y. 2021.** Microbiota Dynamics of Mechanically Separated Organic Fraction of Municipal Solid Waste during Composting. *Microorganisms* **9**:1877. DOI 10.3390/microorganisms9091877.
- Vance N, Brooks JP, Fong SS. 2017.** Metabolic Profile of the Cellulolytic Industrial Actinomycete *Thermobifida fusca*. *Metabolites* **7**:57. DOI 10.3390/metabo7040057.

# Figure 1

The lignocellulose contents of Compost-P II and Mycelium-P III

(Lignocellulose: cellulose, hemicellulose, lignin. Compost-P II: end of the compost; Mycelium-P III: *A. bisporus* mycelia could grow all over the compost after 18 days) .(\* $p < 0.05$ , \*\* $p < 0.01$ ) ( $n=3$ ).

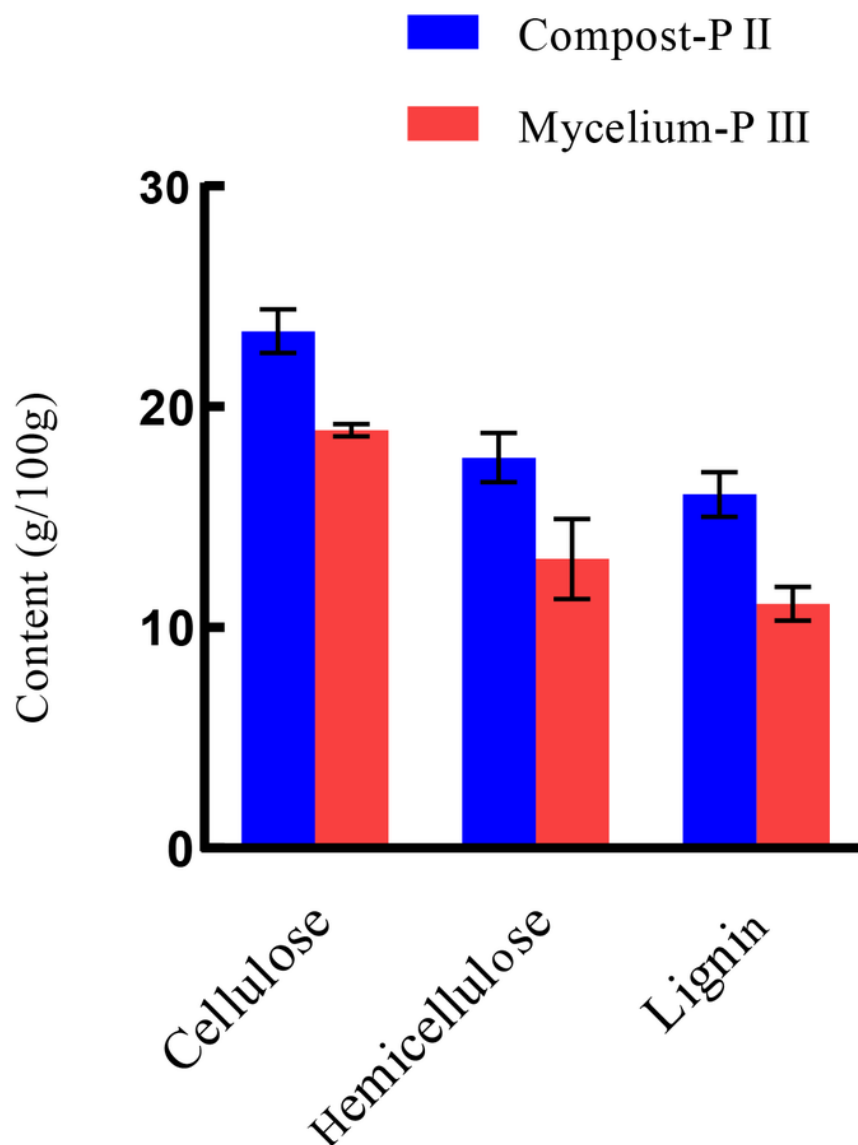


# Figure 2

Enzyme activities in various stages.

(A)FPA activity; (B)xylanase activity; (C)laccase activity; (D)protease activity. (Note:  $*P < 0.05$ .  $**P < 0.01$ .  $***P < 0.001$ .  $****P < 0.0001$ .)

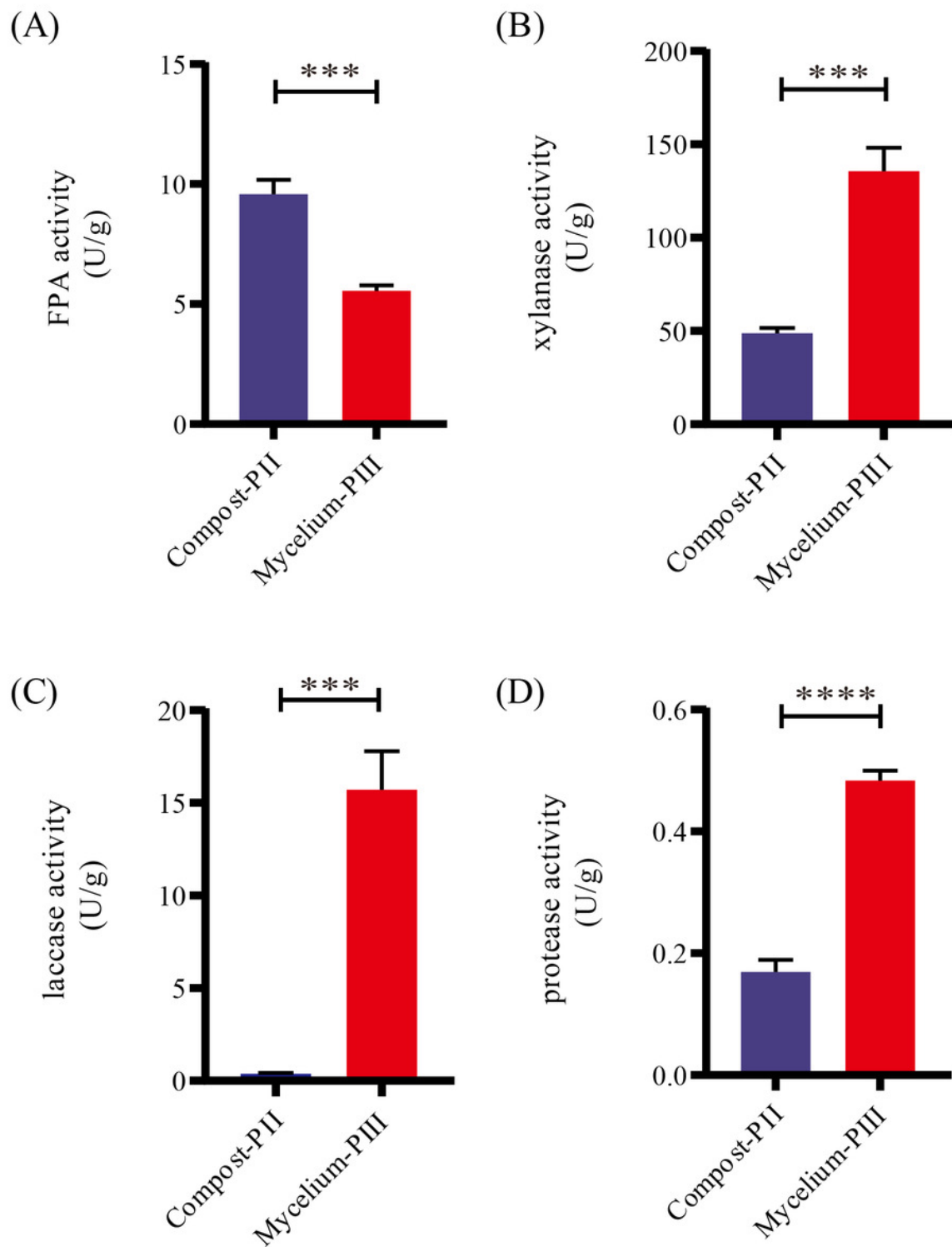




# Figure 3

Microbial community analysis of Compost-P11 and Mycelium-P111 (phylum level).

(A)Relative abundance of microbial communities (Top 10 phyla level). (B)Relative abundance of Ascomycota and Basidiomycota (phylum level).

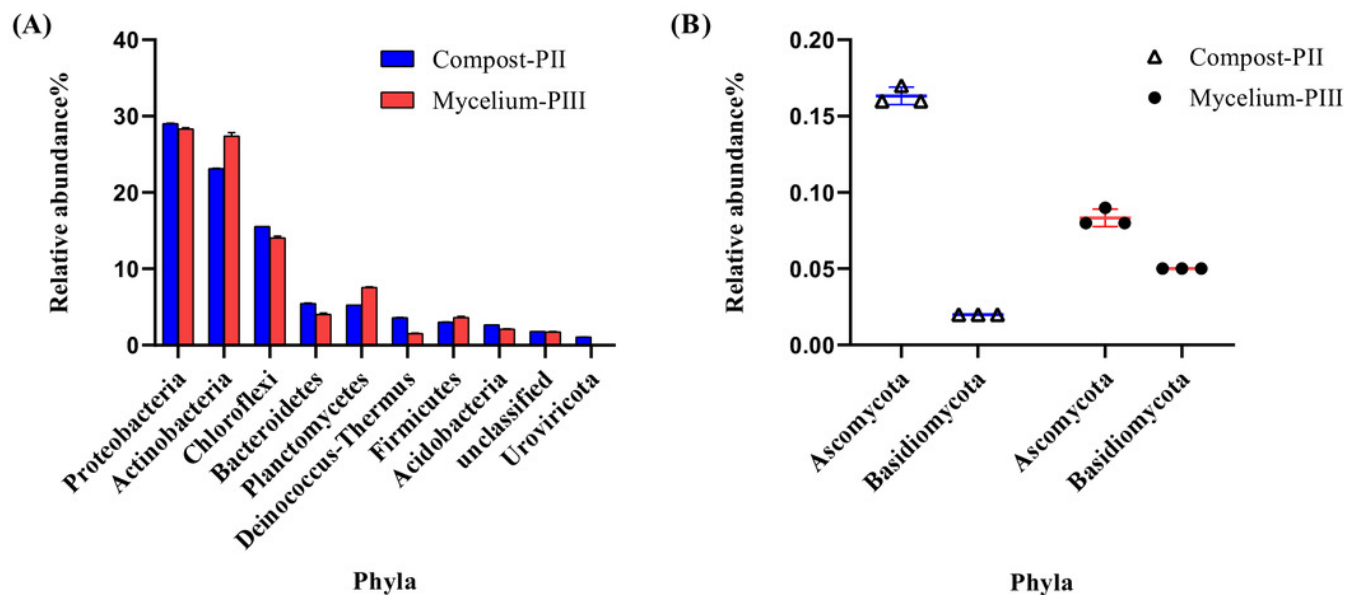


# Figure 4

Significant differences between fungal and bacterial communities for compost-P11 and mycelium-P111 on the genus level

(A:bacterial community; B:fungal community) and species level (C):bacterial community; D:fungal community).

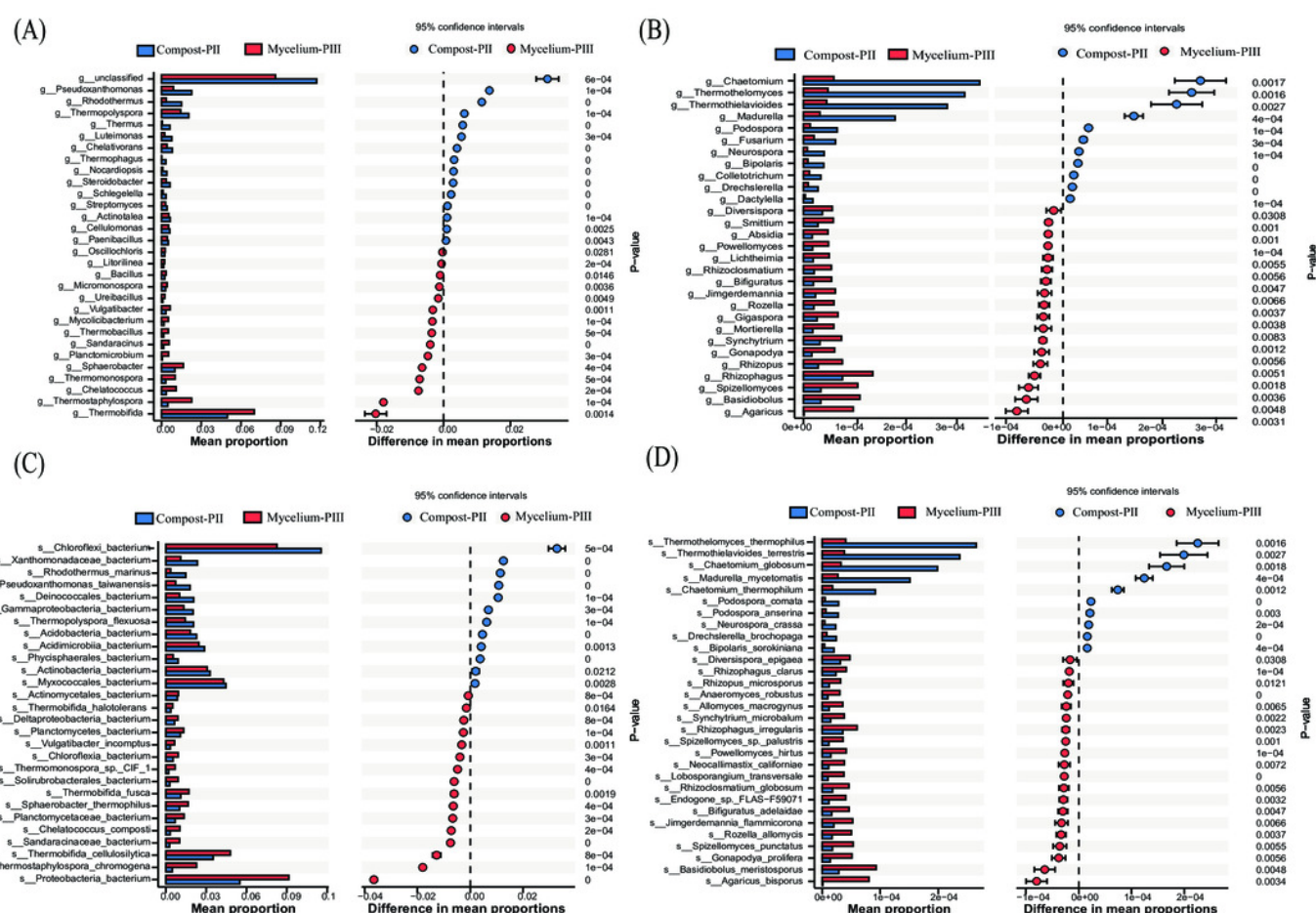


# Figure 5

Differentiated analysis of enzyme families

(A) Difference of putative carbohydrate-activite enzymes of two groups samples. (B) Sankey plots for AA10 in compost-Pll. (C) Sankey plots for AA10 in mycelium-Plll.(D) Sankey plots for cbm13 CBM13 in compost-Pll. (E) Sankey plots for CBM13 in mycelium-Plll.

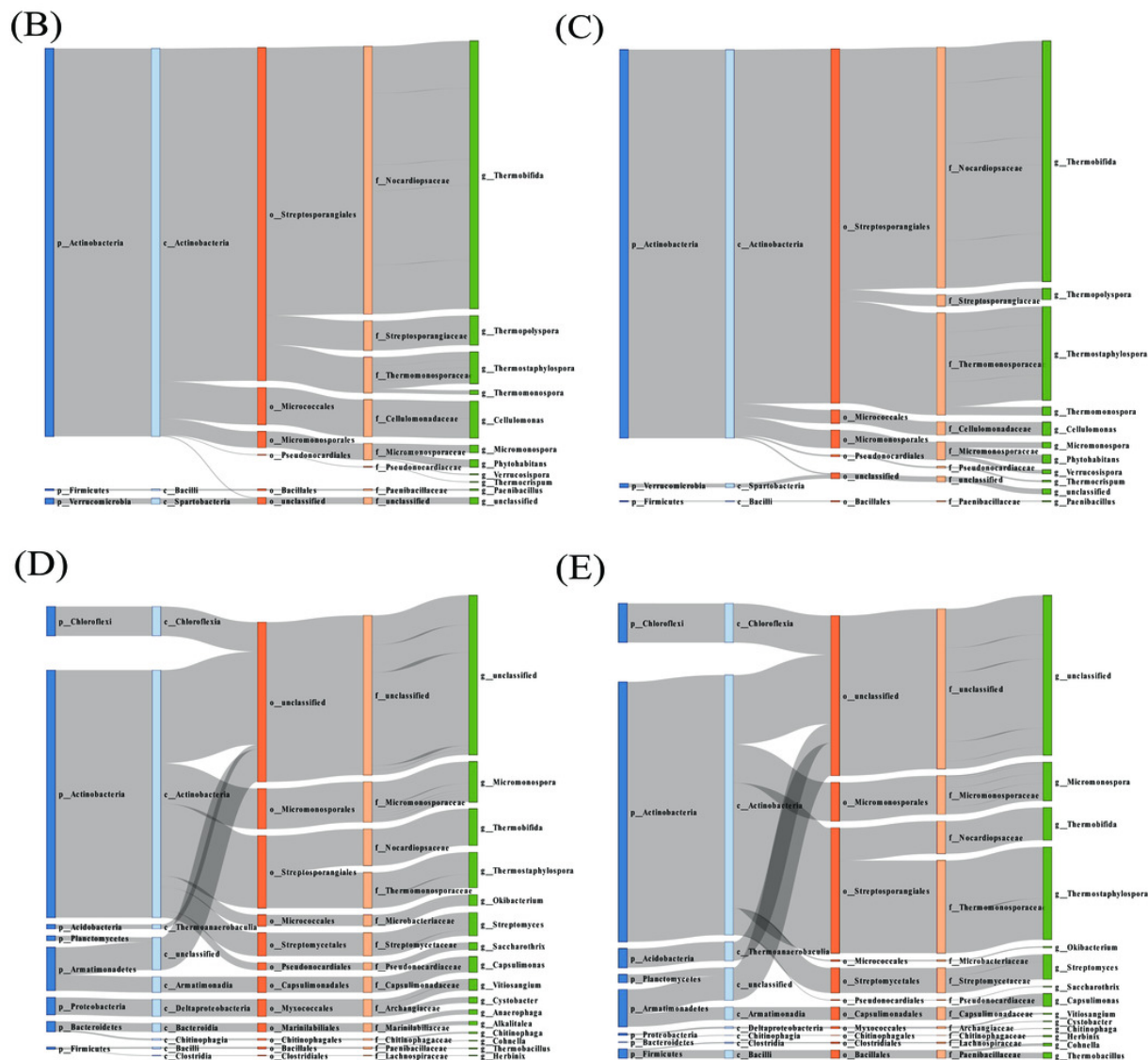
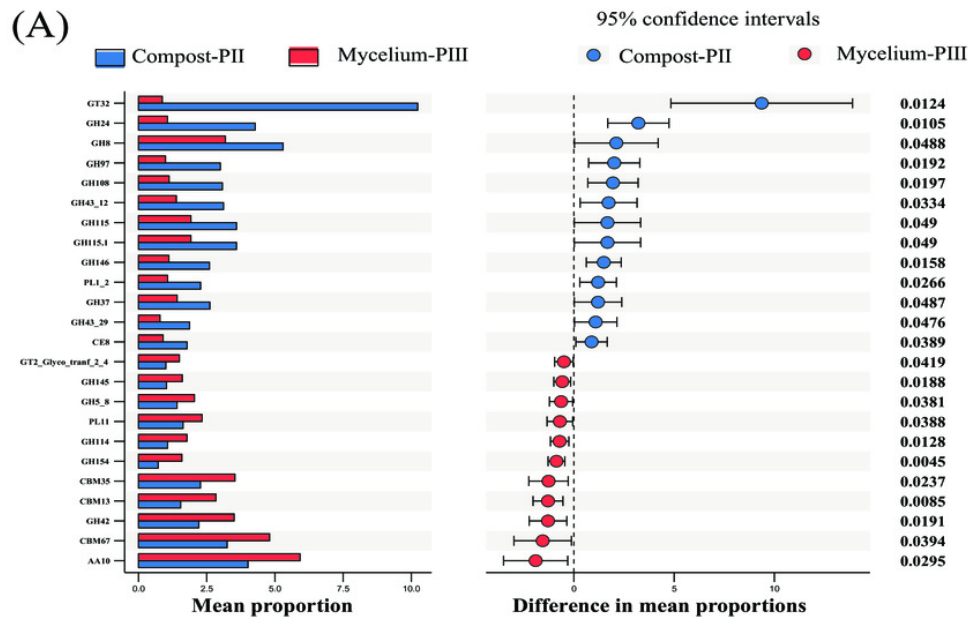


**Table 1**(on next page)

Physicochemical properties of Compost-PII and Mycelium-PIII

Notes. T1,T2,T3: different trials; Results represent mean±standard deviation(n=3).

1 Table 1 Physicochemical properties of Compost-PII and Mycelium-PIII

Phase		Total carbohydrates(w/w%)	Total nitrogen(w/w% )	Moisture(%)	Ash(%)	pH
Compost-P II	T 1	28.48±0.20	2.12±0.03	66.46±0.60	33.6±1.69	7.85±0.09
	T 2	28.63±0.18	2.14±0.07	66.11±0.25	33.54±1.06	7.65±0.25
	T 3	28.58±0.06	2.18±0.08	66.95±1.74	33.96±0.79	7.90±0.20
Mycelium-P III	T 1	23.59±0.22	2.05±0.02	59.50±4.14	36.00±1.22	6.30±0.01
	T 2	23.74±0.15	2.06±0.02	61.80±0.86	36.20±1.36	6.24±0.02
	T 3	23.44±0.28	2.13±0.06	63.00±1.47	34.10±2.61	6.30±0.04

2 Notes. T1,T2,T3: different trials; Results represent mean±standard deviation(n=3).

3

## Table 2 (on next page)

Enzyme family identified in the metagenome.

“↑” and “↓” indicate the up-regulation and down-regulation of the relative abundance for differential CAZy, “-” indicate that there is no difference between the two comparison groups.

1 Table 2 Enzyme family identified in the metagenome.

CAZy family	Annotation	Genes_Count	Total putative CAZy genes, ≥50% Covered Fraction	Total putative CAZy genes, 50-70% Covered Fraction	Total putative CAZy genes, ≥90% Covered Fraction
Cellulose degrading					
GH5(-)	endo-beta-1,4-glucanase ;cellulase	73	50	19	0
GH6(-)	endoglucanase; cellobiohydrolase	31	26	4	19
GH8(↓)	chitosanase ;cellulase;licheninase	60	49	13	31
GH9(-)	endoglucanase ; endo-beta-1,3(4)-glucanase	152	94	21	47
GH12(-)	endoglucanase ; xyloglucan hydrolase	38	36	0	33
GH140(-)	apiosidase	41	24	8	9
GH44(-)	endoglucanase , xyloglucanase	24	15	5	9
GH116(-)	beta-glucosidase ;beta-xylosidase	24	14	4	8
GH3(-)	beta-glucosidase ; xylan 1,4-beta-xylosidase	471	382	87	222
GH48(-)	endo-beta-1,4-glucanase ;chitinase	13	4	1	2
Hemicellulose degrading					
GH10(-)	endo-1,4-beta-xylanase ;endo-1,3-beta-xylanase	223	168	56	78
GH11(-)	endo-beta-1,4-xylanase ;endo-beta-1,3-xylanase	35	31	3	27
GH1(-)	beta-glucosidase; beta-galactosidase	217	136	34	72
GH42(↑)	beta-galactosidase; alpha-L-arabinopyranosidase	60	31	13	10
GH2(-)	beta-galactosidase ; beta-mannosidase; beta-glucuronidase; alpha-L-arabinofuranosidase	151	81	66	7
GH26(-)	beta-mannanase; beta-1,3-xylanase	67	32	0	14
GH27(↓)	alpha-galactosidase; alpha-N-acetylglactosaminidase	10	6	6	0
GH3(-)	beta-glucosidase; xylan 1,4-beta-xylosidase; beta-glucosylceramidase	471	382	87	222
GH31(-)	alpha-glucosidase; alpha-galactosidase; alpha-mannosidase; alpha-1,3-glucosidase	164	102	36	54



GH38(-)	alpha-mannosidase	64	55	15	32
GH39(-)	alpha-L-iduronidase; beta-xylosidase	196	108	85	5
GH4(-)	maltose-6-phosphate glucosidase; alpha-glucosidase	79	69	11	52
GH43(-)	beta-xylosidase; alpha-L- arabinofuranosidase; xylanase	5	2	0	1
GH5(-)	endo-beta-1,4-xylanase; beta- glucosidase; beta-mannosidase	73	50	19	0
GH53(-)	endo-beta-1,4-galactanase	19	15	4	5
GH92(-)	mannosyl-oligosaccharide alpha-1,2- mannosidase; mannosyl- oligosaccharide alpha-1,3- mannosidase	62	30	14	13
GH30(-)	endo-beta-1,4-xylanase; beta- glucosidase; beta-glucuronidase	19	11	3	7
CE1(-)	acetyl xylan esterase; cinnamoyl esterase	730	663	244	163
CE4(-)	acetyl xylan esterase; chitin deacetylase	623	589	87	251
CE7(-)	acetyl xylan esterase; cephalosporin- C deacetylase	123	74	22	33
CE15(-)	4-O-methyl-glucuronoyl methylesterase	111	101	36	51
CE6(-)	acetyl xylan esterase	23	22	2	20
GH78(-)	alpha-L-rhamnosidase	165	60	28	24
GH28(-)	polygalacturonase; alpha-L- rhamnosidase	39	22	11	7
GH35(-)	beta-galactosidase; beta-1,3- galactosidase	34	25	12	11
PL1(↑)	pectate lyase; pectin lyase	9	9	0	2
PL9(-)	pectate lyase	76	22	11	1
CE8(↓)	pectin methylesterase	16	8	5	3
CE12(-)	pectin acetylesterase; acetyl xylan esterase	20	20	1	16
GH18(-)	chitinase; lysozyme	129	77	30	21
GH19(-)	Chitinase; lysozyme	22	9	6	2
GH3(-)	beta-glucosidase; xylan 1,4-beta- xylosidase; beta-glucosylceramidase	471	382	87	222
CE4(-)	acetyl xylan esterase; chitin deacetylase	623	589	87	251
GH13(-)	alpha-amylase; pullulanase	77	59	15	28

GH23(-)	lysozyme type G; chitinase	568	539	93	22
GH51(-)	endoglucanase; endo-beta-1,4-xylanase; beta-xylosidase	118	62	20	0
GH67(-)	alpha-glucuronidase; xylan alpha-1,2-glucuronidase	58	30	8	13
GH127(-)	beta-L-arabinofuranosidase ; 3-C-carboxy-5-deoxy-L-xylose	56	31	9	18
GH32(-)	endo-inulinase;	43	38	10	20
GH97(↓)	glucoamylase; alpha-glucosidase; alpha-galactosidase	41	21	9	11
GH16(-)	licheninase	106	94	24	42
GH29(-)	alpha-L-fucosidase; alpha-1,3/1,4-L-fucosidase	65	48	14	14
GH95(-)	alpha-L-fucosidase ; alpha-1,2-L-fucosidase; alpha-L-galactosidase	53	30	13	13
GH94(-)	cellobiose phosphorylase ;laminaribiose phosphorylase	54	29	15	2
GT35(-)	glycogen or starch phosphorylase	162	92	69	11
Lignin degrading					
AA1(↓)	Laccase /ferroxidase	1	0	0	0
AA2(-)	manganese peroxidase ; versatile peroxidase ;lignin peroxidase	39	12	1	7
AA3(-)	cellobiose dehydrogenase;glucose 1-oxidase	201	122	119	0
AA5(-)	alactose oxidase;glyoxal oxidase ; alcohol oxidase	8	0	0	0
AA6(-)	1,4-benzoquinone reductase	98	86	10	61
AA7(-)	glucooligosaccharide oxidase; chitoooligosaccharide oxidase	405	140	68	49
AA10(↑)	lytic chitin monooxygenase	22	21	0	20

“↑” and “↓” indicate the up-regulation and down-regulation of the relative abundance for differential CAZy, “-” indicate that there is no difference between the two comparison groups.